The International Journal of Advanced Manufacturing Technology (2024) 131:5905–5921
https://doi.org/10.1007/s00170-024-13338-9

ORIGINAL ARTICLE

Wettability and microstructural evolution of copper filler in W and EUROFER brazed joints

Ignacio Izaguirre[1] · Javier de Prado[1] · María Sánchez[1,2] · Alejandro Ureña[1,2]

Received: 20 November 2023 / Accepted: 20 February 2024 / Published online: 5 March 2024

Abstract
In terms of wettability, active systems are characterized by a reduction in interfacial energy as the time at specific conditions is increased. This article aims to investigate the evolution of wettability and microstructure, which undergoes a critical transformation at temperatures and dwell times near brazing conditions due to their significant impact on resultant mechanical properties. The objective is to enhance wettability and prevent the formation of different phases that can occur rapidly within the brazing window conditions. Up to 1105 °C, complete fusion of the filler does not occur. However, once it happens, the expansion of the copper filler in EUROFER increases up to 400%, and the contact angle reduces from 100° to 10°, indicating an active wetting behavior. On the other hand, when copper is used with tungsten, an inert behavior is observed, maintaining the contact angle around 70°. Brazed joints carried out under the most promising wetting conditions demonstrated that at 1110 °C-1 min, various phenomena began to occur. This includes solid-state diffusion of copper in the EUROFER, following the austenitic grain boundaries, and partial dissolution of Fe in the copper braze. Increasing the brazing time from 2 to 5 min achieved high interfacial adhesion properties and controlled the diffusion layer and Fe-rich band formed at the W-braze interface, resulting in the best mechanical results (295 MPa).

Keywords EUROFER · Tungsten · Fusion reactor · Wettability · Brazing

1 Introduction

The escalating energy demands in recent years underscore the necessity of developing fusion reactors as a sustainable energy source. The complexity of the reactor makes it essential to study the various elements comprising its different components. Among the materials considered, tungsten emerges as the most promising option for the first wall and divertor due to its favorable thermophysical properties when confronting plasma [1]. In addition, the martensitic steel, EUROFER, is an ideal choice for application as a structural material in the aforementioned components, owing to its exceptional structural properties and composition [2].

The join of both materials can be achieved by means of different techniques such as soldering [3], brazing [4], or solid-state process [5]. Among these, brazing stands out as one of the most promising techniques for this purpose, as it enables the joining of base materials at lower temperatures than their respective melting points. By using an intermediate filler with a lower melting range, the base materials are better protected from heat damage and preserved during the joining process.

In terms of brazeability, the melting point of the materials to be joined plays a crucial role. This is because the mechanical and chemical properties of materials are directly proportional to their cohesive energies, which increase as the melting point also does [6]. Therefore, an importance effort must be done in selecting of the appropriate filler alloy [7]. In addition, achieving a reliable joint between both materials is crucial. Particularly in heterogeneous joints, there are challenges to overcome, such as controlling thermal stress during operation due to the different coefficients of thermal expansion (CTE) of the base materials. This aspect was studied by Huang et al. [8] who analyzed the strength of diffusion bonding joints between oxide-dispersion-strengthened

✉ Ignacio Izaguirre
ignacio.izaguirre@urjc.es

[1] Materials Science and Engineering Area, ESCET, Universidad Rey Juan Carlos, C/Tulipán S/N, 28933 Móstoles, Madrid, Spain

[2] Instituto de Tecnologías Para La Sostenibilidad, Universidad Rey Juan Carlos, C/ Tulipán S/N, 28933 Móstoles, Madrid, Spain

tungsten and CuCrZr, showing values of up to 200 MPa in high shear strength tests. Additionally, Quian et al. [9] investigated the creep-fatigue behavior of a heat sink in a W/CuCrZr divertor target, developing a model that provides a theoretical basis and guidance for the divertor engineering design of future fusion reactors like DEMO.

In this work, a pure copper filler is employed as an intermediate material to join tungsten with EUROFER. This filler has been widely used by various researchers, demonstrating its suitability for applications in different heterogeneous joints, wherein at least one base material is a Fe-based alloy. This is presented as an alternative despite its high melting temperature due to the good properties of ductility and adaptability, not presenting alloying elements that could form intermetallic compounds that could weaken the joint. For instance, Li et al. [10] successfully utilized a combination of copper and aging treatment to achieve joints with excellent strength and toughness properties. Zhang et al. [11] designed and fabricated dissimilar brazed joints between tungsten and fusion-relevant materials like EUROFER or oxygen-free high thermal conductivity (OFHC) Cu and SS316L steel using a Cu-based brazing foil, resulting in a good metallic continuity. Additionally, Bachurina et al. [12] employed pure copper for joining steel to tungsten and after subjecting the joints to 50 thermocycles (700 °C–water quenching), no failure occurred, although some microstructural degradation was observed after the tests.

Wettability plays a fundamental role in the success of the brazing technique. A favorable wetting behavior between the filler and the base material is essential to ensure complete filling of the joint clearance, thereby averting the occurrence of brazing defects such as porosity or lack of metallic continuity at the joint interfaces. Simultaneously, optimal wettability induces the exudation of the filler material from the joint clearance, resulting in the formation of a thin interlayer at the braze joints. The management of this interlayer is crucial and should be tailored according to the specific service requirements of the joint. Various studies have explored the analysis of this phenomenon, with Seltzman et al. [14] demonstrating the efficacy of copper as an intermediate layer in enhancing wettability. Their findings revealed that the presence of copper inhibited the formation of precipitates at the interface, thereby facilitating the flowability of the filler material. In a related exploration, Lei et al. [15] investigated the impact of brazing temperature on wettability, microstructure, and mechanical properties in the context of YAG ceramic and Kovar alloy using an Ag–Cu-Ti filler alloy [15]. Their research examined the influence of brazing temperature on the diffusion of the (Fe,Ni)Ti reaction layer to the filler metal, leading to the formation of a banded structure comprised of Fe_2Ti–Ni_3Ti phases. This structural transformation contributed to a reduction in shear resistance and nanohardness values.

The investigation of the microstructural evolution of brazed joints is crucial in determining the mechanical properties of the joint. Wu et al. [16] conducted a comprehensive study on the mechanical properties of brazing high-entropy alloys and stainless steels using multilayer nanofoils. The phases formed at the interface primarily encompass Al-Ni-rich body-centered cubic structures and Co-Cr-Fe-rich face-centered cubic structures. Particularly, the phase composition and morphology of the brazed joint undergo alterations based on the conditions of the brazing process, thereby modifying the mechanical properties.

Specifically, prior research on steel-tungsten joints brazed with copper fillers has revealed the formation of brittle intermetallic phases at the tungsten interface [13]. These phases have been meticulously characterized, revealing their substantial impact on the mechanical performance of the joint, especially under thermal fatigue conditions due to the pronounced mismatch in CTE. The system undergoes significant microstructural transformations at the studied temperature over a brief period, necessitating a deep understanding of the formation and evolution mechanisms due to their intense influence on the mechanical properties.

When brazing is utilized as a joining technique, one of the primary considerations is the formation of various phases at the brazed interface. These phases can hinder interdiffusion at the interface or lead to the creation of brittle or intermetallic compounds, resulting in a decrease in mechanical properties during service operation. This issue has been extensively studied by various researchers, including Behzad et al. [16], who investigated how diffusion brazing of IN718/AISI 316L affected the formation of dissimilar joints and its impact on mechanical properties. Li et al. [17] conducted an analysis of the microstructure evolution of a TiAl/GH536 joint that was vacuum brazed with Ti-Zr-Cu-Ni filler metal. They observed the formation of three distinct regions in the joints after brazing: the isothermal solidification layer, continuous reaction layer, and continuous diffusion layer. The microstructural evolution of each phase was found to play a critical role in determining the subsequent mechanical performance of the joint. Finally, Paidar et al. [18] made modifications to the holding time during the brazing process of Inconel617 and stainless steel, introducing an Ag interlayer. They discovered that extending the brazing time to 60 min resulted in a joint with the maximum shear strength of 322.9 MPa, representing a 26% improvement compared to the joint processed at 30 min.

These studies emphasize the importance of not only selecting the appropriate filler but also determining the suitable brazing conditions to achieve the desired microstructure. In systems where the microstructure evolves rapidly, it becomes essential to conduct detailed studies at different temperatures to obtain a microstructure that enhances mechanical properties such as toughness or ductility.

The objective of this article is to investigate the microstructure evolution of a tungsten to EUROFER brazed joint using copper as the filler material. The two main parameters, time and temperature, will be modified to understand the mechanism of braze formation, its impact on braze wettability, and to prevent the formation of undesirable phases that could adversely affect its application in high-temperature scenarios.

2 Experimental details

2.1 Materials

The base materials used for the wetting and brazing tests were as follows: (i) pure tungsten (> 99.97%, *Plansee*) and (ii) reduced activation ferritic/martensitic steel (EUROFER) with a chemical composition in wt.% of 0.11C, 8.9Cr, 0.42Mn, 0.19 V, 1.10W, 0.14Ta balanced Fe and with the following heat treatments 979 °C/1 h 51 min/air cooled plus 739 °C/3 h 42 min/air cooled [19, 20]. The filler used was pure Cu (> 99.9%) supplied by *Lucas Milhaupt* in strip form of 50 µm thick.

2.2 Wettability measurements

To comprehend the wetting behavior of copper in both base materials, various wetting times and temperatures, simulating the brazing tests, were analyzed to understand the influence of these parameters on the studied phenomenon. Contact angle measurements were conducted by recording the melting process inside the furnace using a high-resolution camera, and the contact angles were then determined from the droplet profiles. The filler spreading capability was assessed by measuring the surface area of the filler before and after melting. As a result, specific conditions covering the entire process were selected to represent the wetting process (see Table 1). The spreading of the molten filler was measured, and its microstructure was analyzed for each condition.

To achieve this, W was sliced from a tungsten rod and EUROFER pieces were cut from a plate. Surface preparation of the base materials involved grinding with silicon papers down to a grit size of P4000. Subsequently, 0.2 g of pure copper filler was placed on both the tungsten and EUROFER substrates. The wetting characterization was carried out in a high vacuum furnace (Navertherm) at a residual pressure of 10^{-6} mbar.

2.3 Brazing process

For the brazing tests, the exposed surfaces of both base materials were ground down using a 4000-grit silicon carbide paper. A copper strip filler with the same dimensions as the exposed base material surface was cut and placed between both specimens. The dimensions of the base materials (tungsten and EUROFER) were blocks measuring $6 \times 6 \times 4$ mm^3.

The brazing cycle was conducted in a high vacuum furnace at temperatures of 1105 and 1110 °C, with dwell times ranging from 1 to 10 min, and heating and cooling rates set at 5 °C/min (Table 1).

Table 1 Conditions of wettability tests and brazing tests

Wettability tests		Brazing tests	
Temperature (°C)	Time (min)	Temperature (°C)	Time (min)
1105	1	1105	5
	2		10
	3	1110	1
	4		2
	5		3
	10		5
1110	1		10
	2		
	3		
	4		
	5		
	10		

2.4 Characterization techniques

Cross sections of the solidified drops and brazed joints were prepared for metallographic examination using the standard polishing technique. The microstructures of the wetting interfaces and brazed joints were analyzed using a stereoscopic microscope (*Leica DFC320*) and scanning electron microscopy (SEM) equipped with energy-dispersive X-ray microanalysis (EDX) on a Hitachi S3400. For a more detailed examination of the microstructure, some samples were etched before microscopic observation. In this case, a solution of 10 ml HNO_3, 30 ml HCl, and 30 ml glycerol was used for EUROFER etching, while 30 ml ammonia, 60 ml hydrogen peroxide (3%), and 30 ml deionized water were used for the braze etching.

The shear strength values were determined utilizing a specialized compression device engineered to maintain precise alignment of the brazed joint with the applied load. This design effectively prevented any undesirable bending of the specimens during testing, thereby ensuring a consistent and pure shear stress on the brazed surface. The custom fixture was carefully positioned between the compression plates of a Universal Testing Machine (*Zwick Z100*), with tests conducted at a controlled displacement rate of 1 mm/min. To enhance the reliability of the results, three samples were

tested under each condition, a measure implemented to minimize deviations from the main value. Vickers microhardness profiles were measured across the W-EUROFER interface using a MHV-2SHIMADZU equipment. A 100 g load was applied for 15 s, and distances between neighboring indentations were kept longer than twice the residual imprint sizes. Three indentation lines were made per distance to reduce the error in the measurements.

3 Results

3.1 Wetting angle measurements of Cu braze on tungsten and EUROFER

The first step in achieving a high-quality joint is to ensure complete filling of the joint clearance. To understand the wetting behavior of the copper filler and the interfacial reactions governing the wetting performance, a comprehensive study of microstructure development and phase formation at each interface is necessary. These factors not only influence wettability but also play a significant role in determining future mechanical performance. Therefore, the expansion and contact angle of the filler in each base material were studied at various temperatures and dwell times. The interfacial microstructure was also evaluated to establish a correlation with wetting observations.

In the initial results, contact angle variations between copper and the base materials were analyzed. The first drop formation was observed at 1105 °C, as lower temperatures did not result in completed drop formation within the studied dwell times, which are not of interest from a brazing standpoint. Considering the rapid evolution of the microstructure at these temperatures, as will be demonstrated later, 1105 °C and 1110 °C were selected for the study, with dwell times ranging from 0 to 10 min. These conditions ensure the investigation of the desired brazing window that provides the necessary microstructure for future joints.

Figure 1 illustrates the evolution of the drop profile of the system at these temperatures, displaying the low contact angle of the copper drop in EUROFER after 10 min at 1105 °C, and the higher angle observed in the tungsten sample, despite the higher temperature used in this case. The first case corresponds to an active system, wherein the interaction of both metallic components progressively decreases the interfacial energy. In contrast, the second case corresponds to an inert system, where, once the equilibrium has been reached, the system remains constant.

Once the copper has melted and formed the droplet, in the case of the copper-EUROFER system, it tends to expand over the EUROFER substrate, covering a large surface area. This behavior is a result of the excellent wettability of copper in steel, a phenomenon that has been extensively studied in plain steel by several authors [21–23]. During the initial moments of the melting process, the expansion reaches up to 400% of the initial area. However, the active behavior of this system allows for continuous expansion of the filler, as shown in Fig. 2a and b. The results demonstrate that as

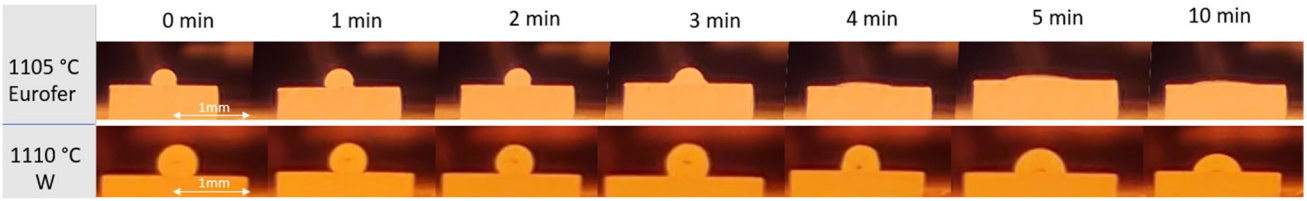

Fig. 1 The variation of the contact angle between copper and the base materials at different temperatures and times

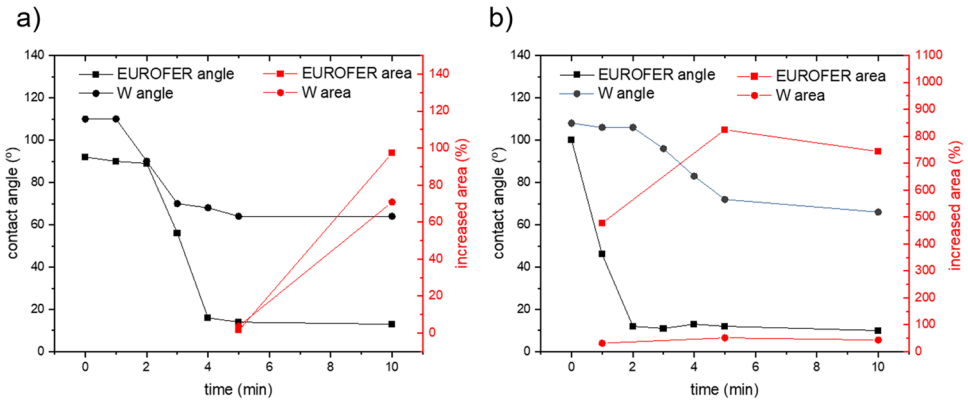

Fig. 2 Wettability studio through the area increase and contact angle of EUROFER and W at **a** 1105 °C and **b** 1110 °C

both time and temperature increase, the filler expansion also increases, reaching values close to 800% at 1110 °C for 5–10 min. Consequently, the in situ measured contact angle is reduced by the application of isothermal treatments or higher temperatures, as shown in Fig. 2. The contact angle reduction is especially significant after 2–3 min at 1105 °C or 1–2 min at 1110 °C, which could be associated with interfacial interactions in this active system. The initial contact angle in this case is close to 90°, but after the mentioned time periods, it is reduced to approximately 10°, indicating a high wettability system.

In the case of tungsten, an initial contact angle of 110° is observed. After 2–3 min, depending on the testing temperature, the angle is reduced to approximately 70º, remaining constant thereafter. The low wettability observed results in a lower filler spreading over the substrate surface, reaching values of 50–70% of the initial filler surface.

Figure 3 visually demonstrates the different wetting behavior of copper in EUROFER and tungsten. Figure 3a and c and Fig. 3b and d show base materials before and after the simulated brazing test, respectively. This figure clearly illustrates the significant difference in the spreading capability between the copper-EUROFER system and the copper-tungsten system.

To understand the active and inert characteristics of both systems, various experiments using the conditions shown in Table 1 were conducted and the microstructure of the solidified drop over the substrate was analyzed by studying the cross-section slide.

Regarding the copper-EUROFER system, the interaction may begin at the very early stages of melting or even when both materials remain in a solid state, as can be deduced from the binary phase diagram (Fig. 6a). The solubility of copper in iron increases with temperature, reaching approximately 8 at. % under the test conditions. Hence, solid-state diffusion is expected to occur at the contact interfaces of both metallic materials.

Figure 4 shows the evolution of the resulting microstructure, with a focus on the interface, for different simulated brazing treatments ranging from 1105 to 1110 °C with varying dwell times. The first condition, 1105 °C for 5 min, already shows interactions between copper and EUROFER (Fig. 4a). As discussed earlier, during the heating process, copper diffuses following a solid-state mechanism, resulting in an enrichment of copper in the closest area of EUROFER. However, the subsequent melting of copper changes the interaction mechanism to one governed by a solid–liquid interface. In this micrograph, iron-rich precipitates can be observed (white square in Fig. 4a), as well as the initial solid–liquid interaction at the interface (squared in Fig. 4a). Both phenomena will be described in detail later on.

Figure 4b–d show the microstructure of the copper-EUROFER joint, revealing different interaction mechanisms. As temperature and dwell times increase, the interaction and diffusion processes are promoted. At the EUROFER interface, with longer simulated brazing times, copper penetrates into the EUROFER following prior austenitic grain boundaries (Fig. 4c and d). This process is linked to the mechanism previously studied and initiated during the heating process when copper diffuses into the EUROFER mainly along grain boundary paths, where diffusion is facilitated [24]. The enrichment in copper could lead, in those areas, to the formation of low melting point phases, where the alloying elements of EUROFER plays and important role [25]. Additionally, the equilibrium phase diagram shows the solubility of Fe, which is 5 wt. % at the melting temperature of copper and continues to increase in the liquid state. Consequently, there is a Fe enrichment in the copper area, and during the cooling process, as solubility decreases, iron precipitates in flower-like geometries, marked with white arrows in Fig. 4c.

All these described reaction processes reduce the solid–liquid interface energy and are responsible for the active behavior of the system and the improvement of wetting behavior. It is expected that as the temperature and time are increased, these processes will continue, leading to further improvements in wettability until an equilibrium in the interface is reached.

In the case of the copper-W system, a completely different behavior is observed. As described in Fig. 2, the initial contact angle in the sample at 1110 °C-1 min is more than 100°, significantly higher than the copper-EUROFER one, resulting in a lower initial expansion of the filler. The filler expansion only shows an initial increase at 1105 °C, which could be attributed to the completion of the melting process

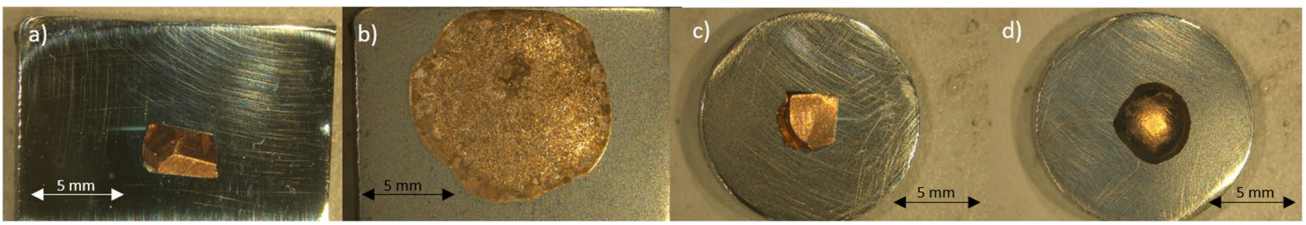

Fig. 3 General view by steroscopic microscope of samples of copper at 1110 °C for 5 min of copper over EUROFER **a** before and **b** after heating, and over W **c** before and **d** after heating

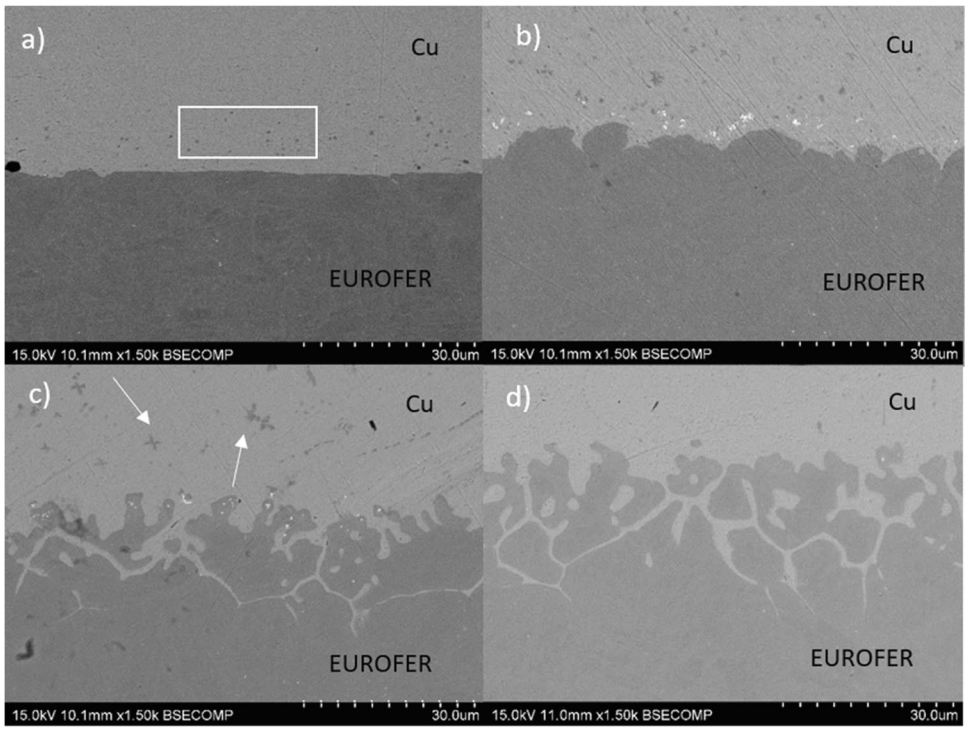

Fig. 4 SEM micrographs of interaction between copper and EUROFER at **a** 1105 °C-5 min, **b** 1110 °C–1 min, **c** 1110 °C-5 min, and **d** 1110 °C-10 min

until reaching equilibrium at the solid–liquid-gas system, which governs the wettability (Fig. 5). Subsequently, no variation in the area is observed. In this case, the lack of solubility of copper in tungsten (Fig. 6b) and the absence of interfacial reactions (Fig. 5a and b) render the system inert at the temperatures and times studied.

3.2 Microstructural characterization of W-EUROFER brazed joints

3.2.1 Brazing test 1110 °C-1 min

Considering the wettability study, brazing of tungsten and EUROFER was conducted using copper as the filler material under similar conditions to those studied in the wettability tests. Based on the wettability results, it was observed that the formation of the copper drop begins to occur at 1105 °C for 5–10 min; hence, the initial attempts used these conditions to braze both materials.

The results of the samples subjected to these conditions are shown in Fig. 7a, indicating a poor joint quality where the metallic continuity is not fully established. Some areas of both brazed interfaces lack metallic content due to inadequate wetting characteristics associated with an incomplete melting process.

However, when the brazing conditions are changed to 1110 °C for 1 min (Fig. 7b), the melting process is completed, and copper is able to fill the entire joint clearance. As a result, full metallic continuity is achieved. Upon closer analysis of both interfaces, partial incorporation of copper into EUROFER is observed in some areas (Fig. 7c). Typically, this process occurs due to the solid-state

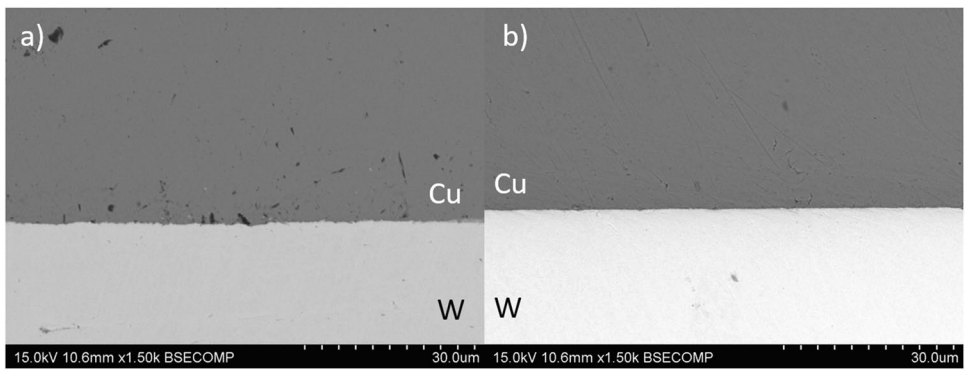

Fig. 5 SEM micrographs of interactions between copper and tungsten at **a** 1110 °C-1 min and **b** 1110 °C-10 min

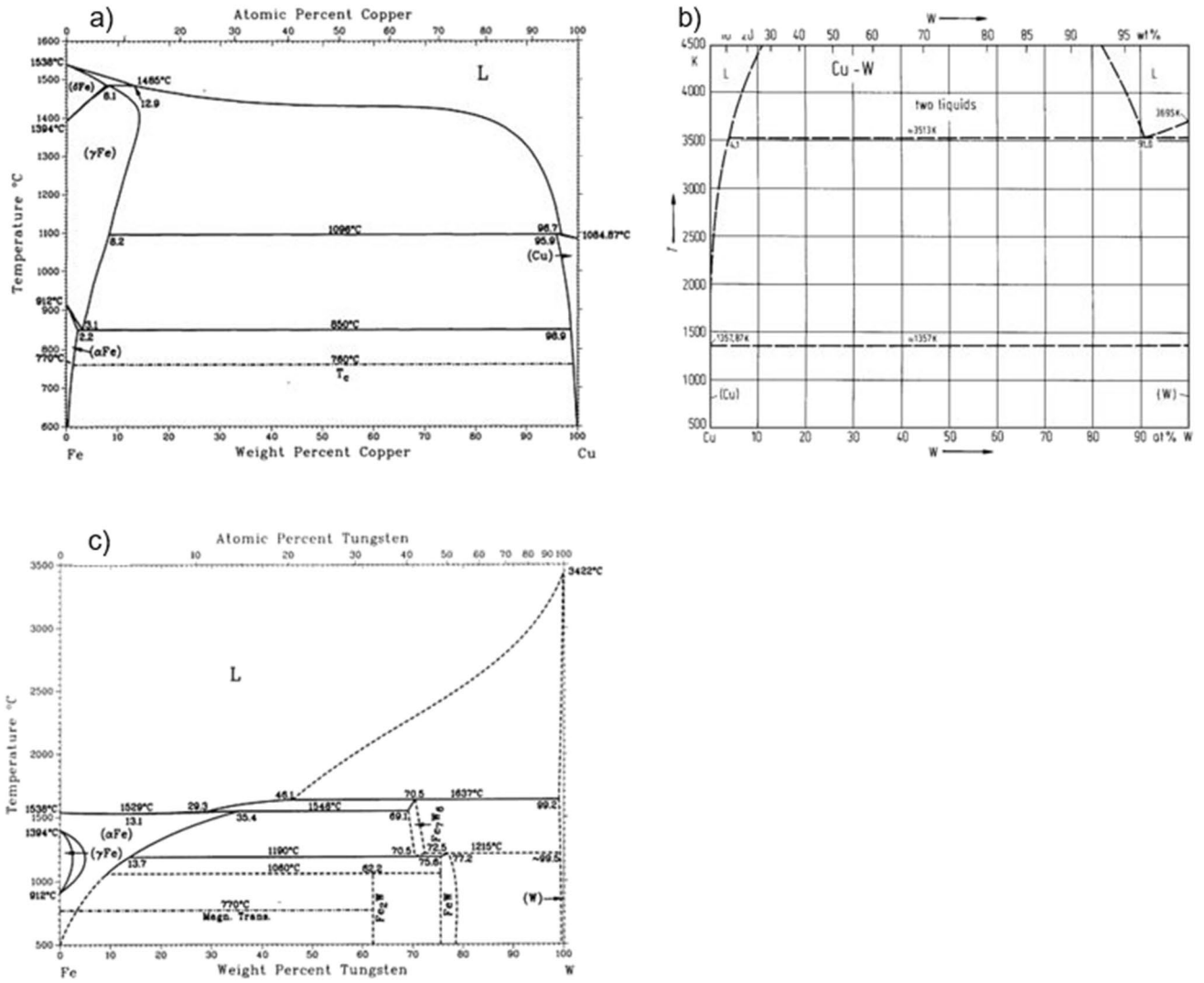

Fig. 6 Binary phase diagram of **a** Cu-Fe, **b** Cu-W, and **c** Fe-W [26]

diffusion of copper in EUROFER along the austenitic grain boundaries (Ac1 = 890 °C) [27], where diffusion is promoted and can occur with a diffusion coefficient several times higher than in bulk materials [28]. The increase in copper solubility in steel as the temperature rises further promotes this phenomenon. After this process, copper can diffuse from the grain boundaries into the inner grains in those zones. In Fig. 7c, the microstructure corresponds to this initial stage of the process, where copper has initiated its penetration into some grain boundaries (white arrows), resulting in enrichments of the surrounding steel grains.

On the contrary, the W-copper interface did not exhibit any interaction between both elements due to the refractory nature of tungsten (Fig. 7d), which inhibits solid-state diffusion phenomena at those temperatures. Additionally, the equilibrium phase diagram does not indicate any miscibility between both elements [26].

3.2.2 Brazing test 1110 °C-2 min

The joint brazed at 1110 °C for two min produces the evolution of the microstructure shown in Fig. 8b. The general micrograph demonstrates good brazeability between both base materials. A detailed micrograph obtained by FEG-SEM of the EUROFER-copper interface is shown in Fig. 8b, where the sample has been etched to provide a clearer understanding of the microstructure. The figure illustrates how copper penetrates through grain boundaries (GB), reaching approximately 5 µm into the steel. Following with the previous explanation for 1110 °C for 1 min samples, the enrichment in copper above explained in the GB along with the typical impurities remained in those zones, which could include MX carbides of the alphagen elements of the steel, could reduce the melting point of those zones by the formation of ternary low temperature

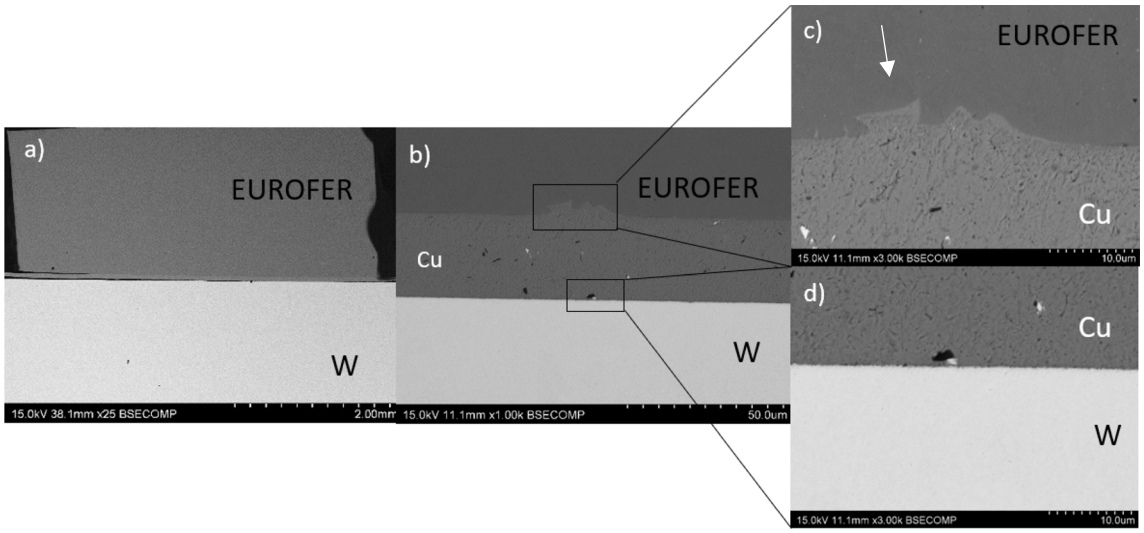

Fig. 7 SEM micrographs of joints after the brazing process of **a** 1105 °C-10 min, **b** 1110 °C-1 min, **c** detail of Cu-EUROFER interface, and **d** W-Cu interface

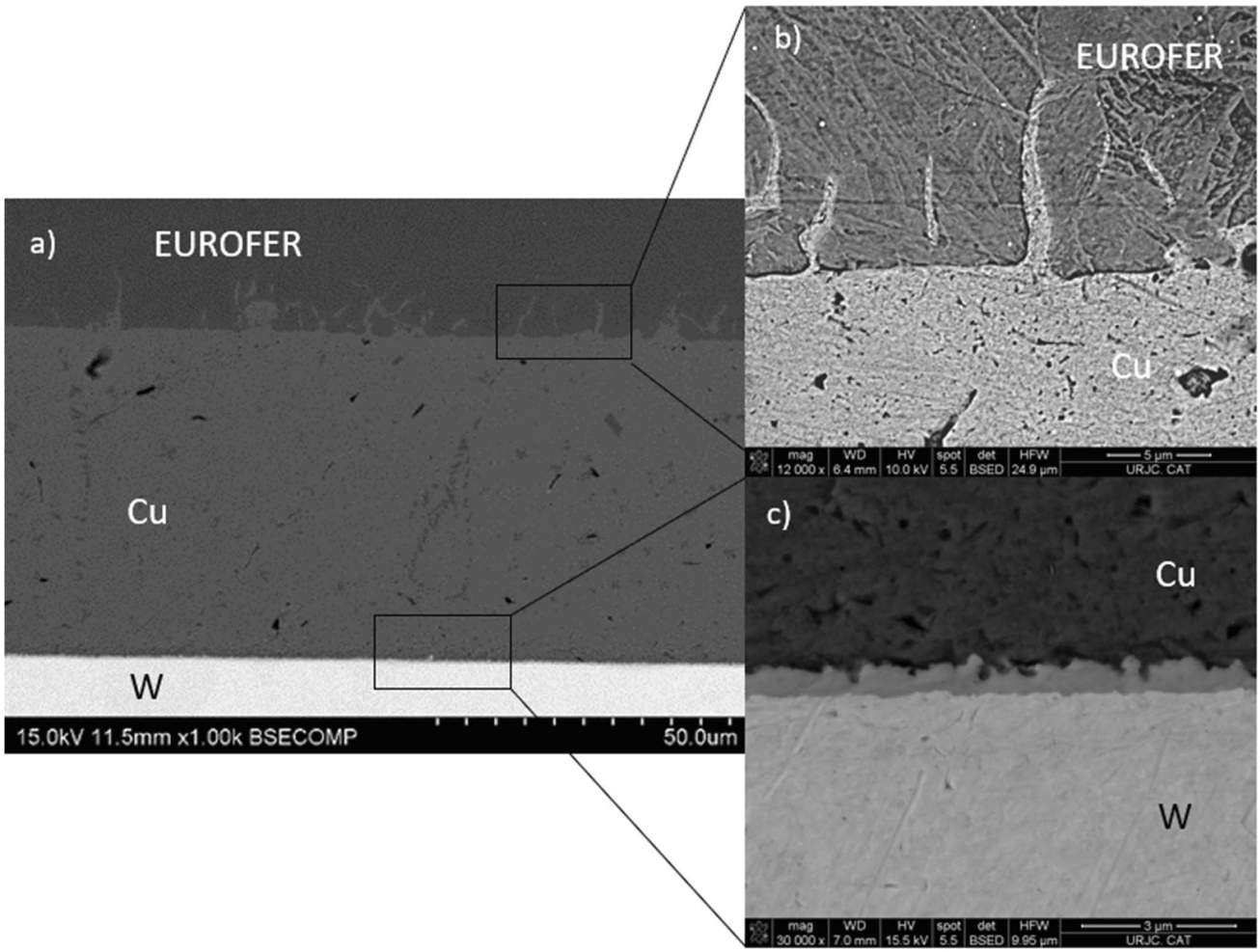

Fig. 8 SEM micrographs of joints **a** after the brazing process of 1110 °C-2 min, **b** detail of Cu-EUROFER interface, and **c** W-Cu interface

eutectic compositions giving rise to grain boundary liquefaction process.

The analysis of the W-filler interface revealed a different microstructure evolution than that described in the wettability study (Fig. 8c). In this case, the formation of a diffusion layer on the top of the W base material, approximately 0.5 µm thick and composed of 39W51Fe9Cr % at. was observed. The formation of this layer can be explained by a solid-state diffusion mechanism, in which iron plays an important role in activating the process.

In Fig. 8b, a more detailed examination of the EUROFER-copper interface, after etching and obtaining elemental mapping composition, revealed the formation of iron dendrites inside the copper filler. The presence of these structures can be attributed to the high solubility of iron in copper at high temperatures, which reaches approximately 3.5 at. % at the brazing temperature (see Fig. 6a). During cooling, iron solubility decreases, and it begins to solidify in the molten copper through a heterogeneous mechanism, resulting in the formation of dendrites. Once the filler has fully solidified, iron solubility continues to decrease almost to zero at room temperature. In this case, iron precipitates with a more spherical geometry inside the filler (red arrows in Fig. 9a and b).

The presence of iron dissolved in copper at the brazing temperature, and subsequently at lower temperatures, enables the formation of the previously explained diffusion layer at the top of the tungsten base material. This formation is promoted by the presence of iron and, therefore, was not observed during the wettability study.

3.2.3 Brazing test 1110 °C-3 min

Extending the brazing time up to 3 min resulted in a higher interaction at the EUROFER-copper interface. The incorporation of copper into EUROFER was enhanced, initially through grain boundary (GB) paths, and later by diffusion into the bulk grain from the GB using solid-state diffusion

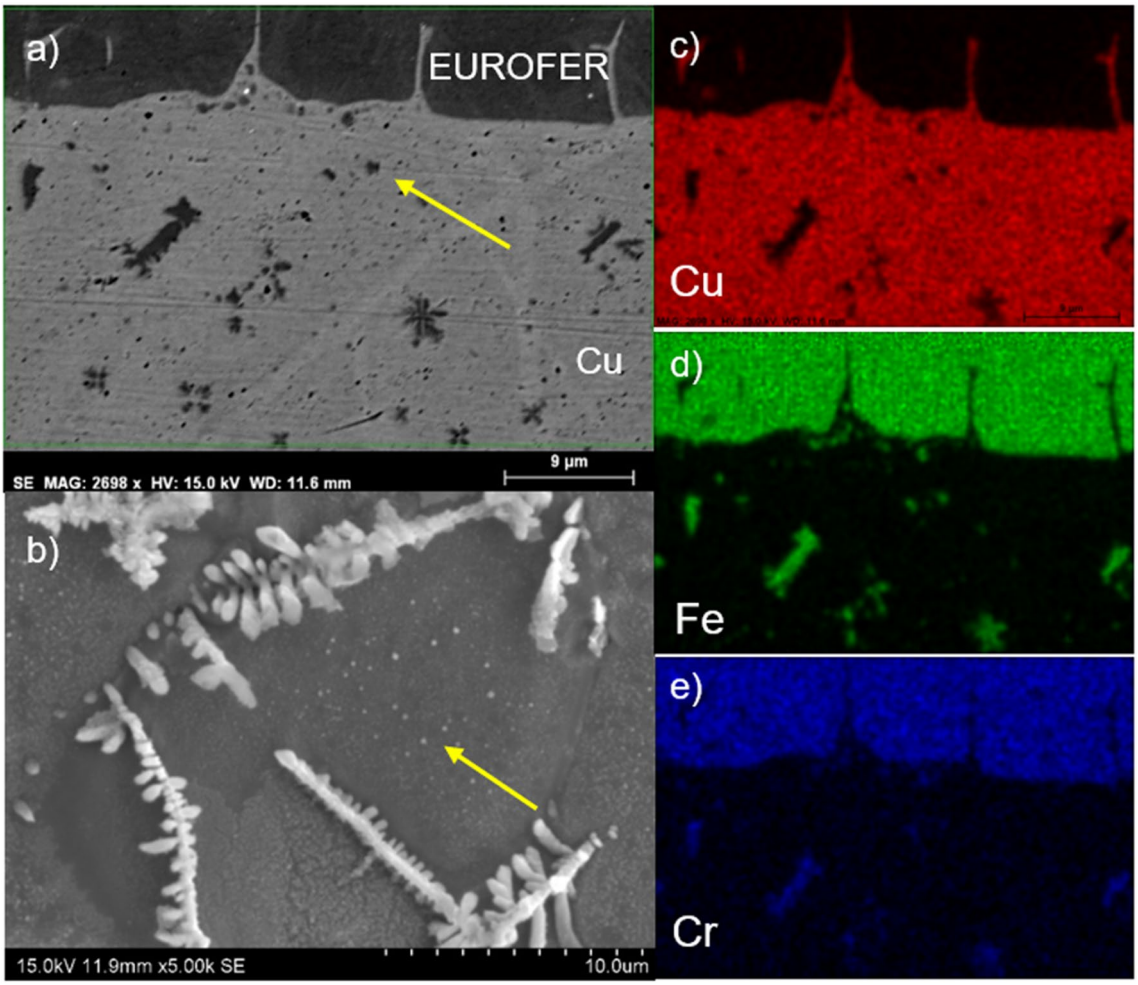

Fig. 9 Detail of iron dendrites in the brazing condition 1110 °C-2 min: **a** SEM image, **b** after copper was etched, and **c–e** elemental distribution map of Cu, Fe, and Cr at the Cu-EUROFER interface

mechanisms. Additionally, the phenomenon of grain boundary liquefaction was observed, leading to the formation of ternary or more elements low-temperature eutectic compositions. This facilitated copper penetration up to 20 µm from the interface.

The study of the W-copper interface revealed the formation of a Fe-rich discontinuous layer above the previously explained diffusion layer (Fig. 10). This layer has a composition of 79Fe7W8Cr5Cu at. % according to EDX analysis. The formation of this Fe-rich layer is associated with the increased Fe content in the copper braze as the brazing time also increases, allowing more time for iron to solubilize and increase its concentration in the filler. During cooling, heterogeneous solidification occurred more easily in solid structures due to the lower energy required, which is the tungsten base material in this case. The formation of this layer led to the growth of the diffusion layer from 1 µm in zones where the phase was not observed to 1.9 µm in zones where this

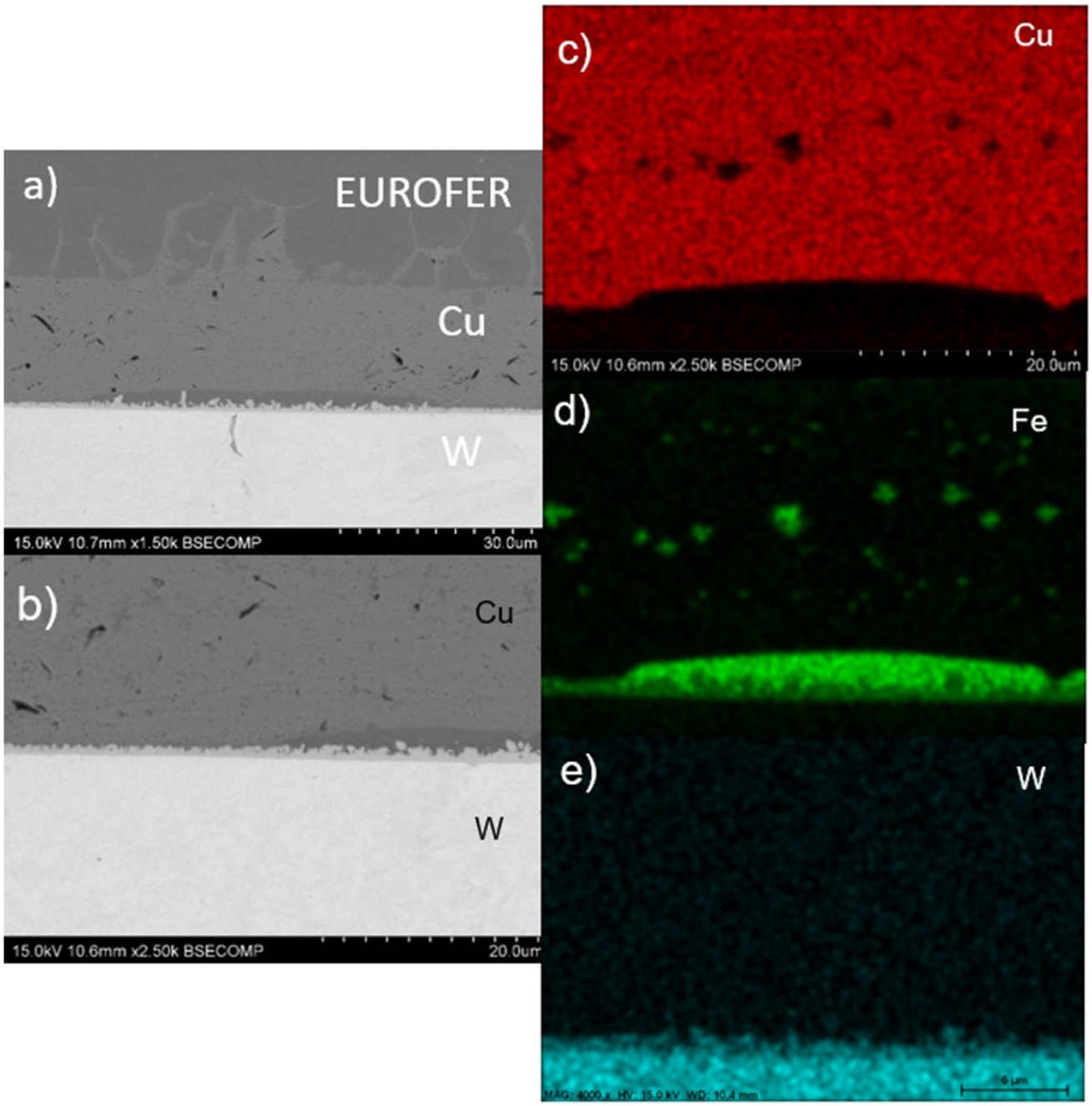

Fig. 10 SEM micrographs of joints **a** after the brazing process of 1110 °C-3 min and **b** detail of W-Cu interface, **c**–**e** elemental distribution map of Cu, Fe, and W at the Cu-W interface

Fe-rich layer was formed above. The higher access of iron to the diffusion layer resulted in this effect.

3.2.4 Brazing test 1110 °C-5 and 10 min

Brazing dwell times at 1110 °C for 5 and 10 min gave rise to a microstructure evolution continuing the above explained interaction mechanisms at the EUROFER-braze interface, where the penetration of copper reached 14 µm for 5 min and 24 µm for 10 min. However, there are some differences that need to be discussed.

The time at this temperature allowed the formation of a continuous Fe-rich layer beneath the copper braze at the edges of the samples, as shown in Fig. 11a and d for 1110 °C-5 min and 10 min, respectively. However, at the center of the joint, the copper braze disappeared, and only the Fe-rich band was observed beneath the remaining copper at EUROFER grain boundaries (Fig. 11b and e for 1110 °C-5 min and 10 min, respectively).

This particular microstructure is associated with the exudation of copper from the joint clearance due to the high wettability observed. As a result, copper accumulated on the edges of the sample, leaving only a thin layer of copper in the center of the joint, which then penetrated through the grain boundaries, as previously explained.

Under these conditions, the formed diffusion layer had a thickness of 840 nm for 5 min and 1.21 µm for 10 min, corresponding to the micrographs shown in Fig. 12c and d, respectively.

In conclusion, the evolution of the microstructure can be explained following the schematic representation shown in Fig. 12. Initially, EUROFER and tungsten are in direct contact with the copper filler. Once the filler is melted, it starts to penetrate into the steel following grain boundaries paths, leading to the grain boundaries liquefaction process due to the formation of low melting point eutectic composition. Simultaneously, a dilution phenomenon of iron into the liquid copper is observed, resulting in the formation, during cooling, of iron dendrites in the copper band (Fig. 12a). As the brazing time is increased, the formation of the diffusion layer on the tungsten interface begins, driven by the solubility of iron in tungsten and the increase of iron concentration in the melted copper braze, which reaches the tungsten-braze interface (Fig. 12b). The excess of iron beyond the solubility limits, as the cooling occurs, leads to the formation of the Fe-rich phase above the diffusion layer, initially as isolated phases and later forming a continuous layer as the dwell time increases (Fig. 12c). At this point, the copper continues its penetration into EUROFER grain boundaries, and the enrichment of copper in the grains nearest the interface continues. This phenomenon, along with the exudation of copper out of the joint clearance, causes the copper braze to become thinner as the brazing time increases (Table 2). Finally, the copper braze thickness is reduced, and it may disappear in some areas in the center of the joint, where the Fe-rich phase forms a continuous layer at the interface, enhancing the growth of the diffusion layer (Table 2).

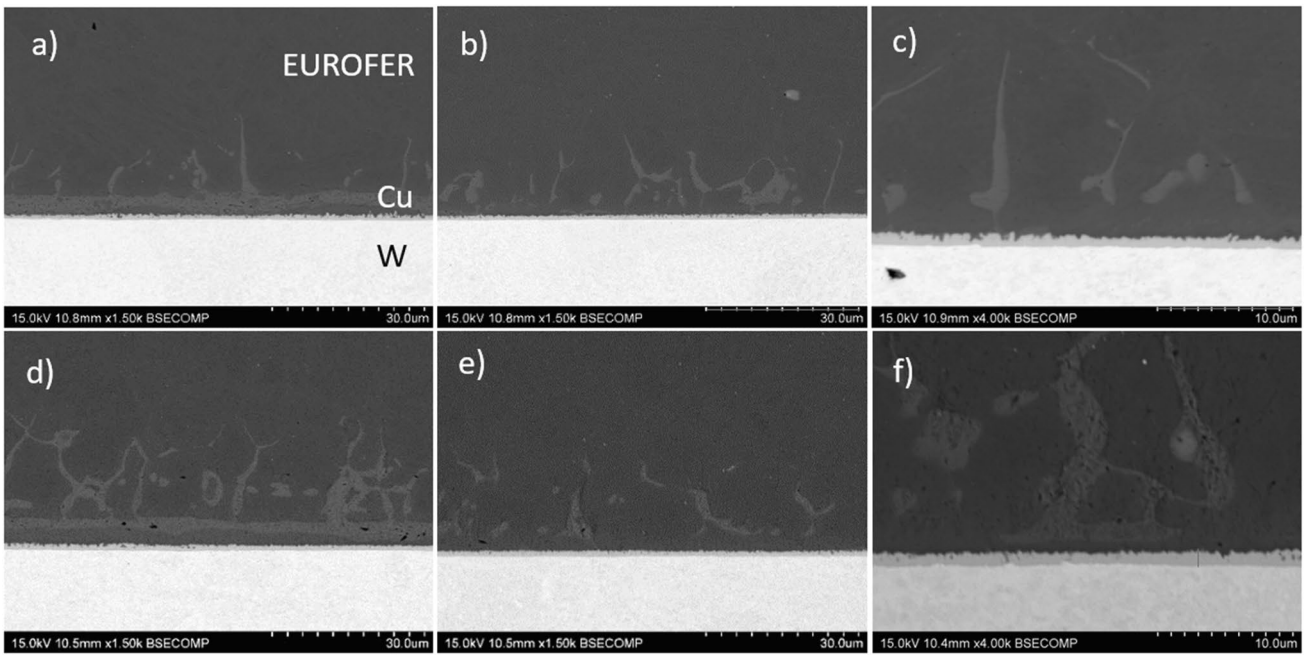

Fig. 11 SEM micrographs of joints after the brazing process of external zones: **a** 1110 °C-5 min and **d** 1110 °C-10 min, center of the sample of **b** 1110 °C-5 min and e 1110 °C-10 min, and details of the diffusion layer **c** 1110 °C-5 min and **f** 1110 °C-10 min

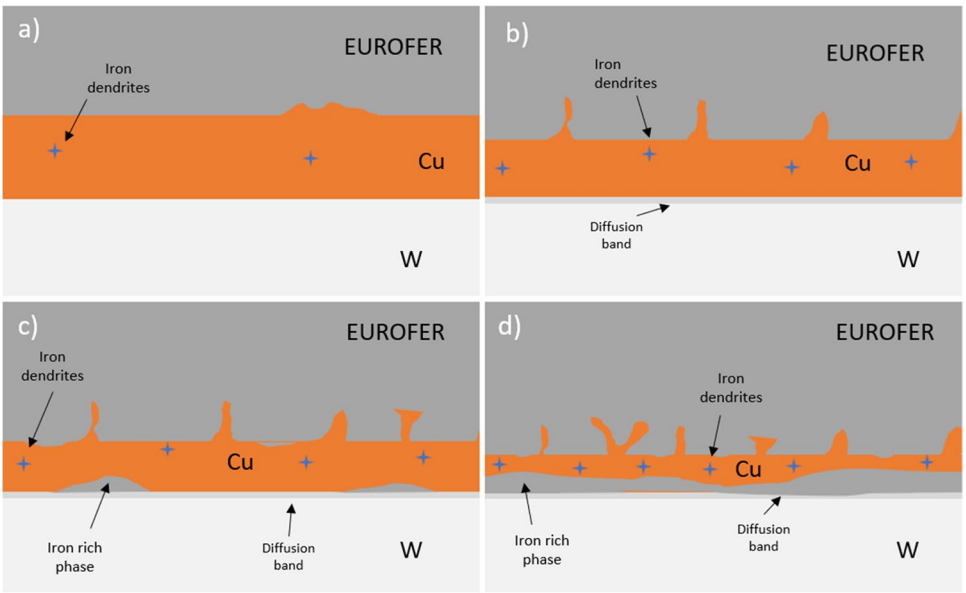

Fig. 12 Schematic representation of the microstructural evolution during the brazing process at 1110 °C **a** 1 min, **b** 2 min, **c** 3 min, and **d** 5 min

Table 2 Resume of how change the characteristics the joint between both materials at 1110 °C

	Diffusion layer thickness (nm)	Copper band thickness (μm)
1110 °C-1 min	-	40
1110 °C-2 min	650	48
1110 °C-3 min	1000	32
1110 °C-5 min	840	10 at the center
1110 °C-10 min	1210	9.5 at the center

3.3 Mechanical characterization

3.3.1 Shear test

The strength of the brazed joints, measured in shear mode, are compiled in Fig. 13. There is a clear influence of the brazing time in the strength of the joints associated to the microstructural changes observed in previous sections. Only brazing temperatures of 1110 °C were chosen for the mechanical characterization due to the poor brazeability of lower temperatures observed.

Samples brazed for 1 and 2 min at 1110 °C showed the poorest values, where the shear strengths were 11 ± 2 MPa and 7 ± 5 MPa, respectively. However, completely different behavior is observed when dwell times of 3 and 5 min were used. Those samples showed shear values of 251 ± 15 MPa and 295 ± 1 MPa, respectively. Finally, the application of the longest brazing time studied showed a reduction of the strength back to 190 ± 60 MPa. The explanation of the results could be analyzed by combining the study of the fracture surface and the microstructural observation of the

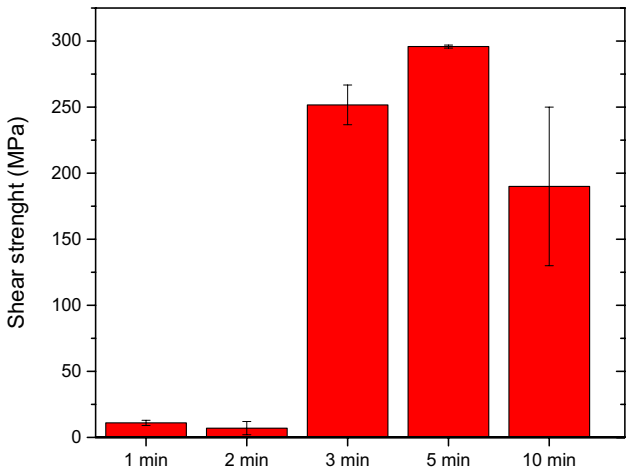

Fig. 13 Shear strength of the W-EUROFER joints at 1110 °C from 1 to 10 min

joint. Fracture of samples brazed for 1 and 2 min gave rise to the decohesion, after plasticization of the copper filler, of both interfaces but, fundamentally, of the W-braze interface due to the low adhesion interfaces formed. Thus, the filler could be clearly observed after the fracture of the joint at low strengths (Fig. 14a).

The application of longer brazing times from 3 to 5 min enhances the interaction mechanisms, such as solid diffusion in both interfaces, which could be evidenced by the formation of the diffusion layer at the W-braze interface and the penetration of copper in the austenitic grain boundaries as it has been explained in the microstructural sections. These phenomena improve the adhesion properties and, as a result, the strength of the joint is clearly improved. Those samples

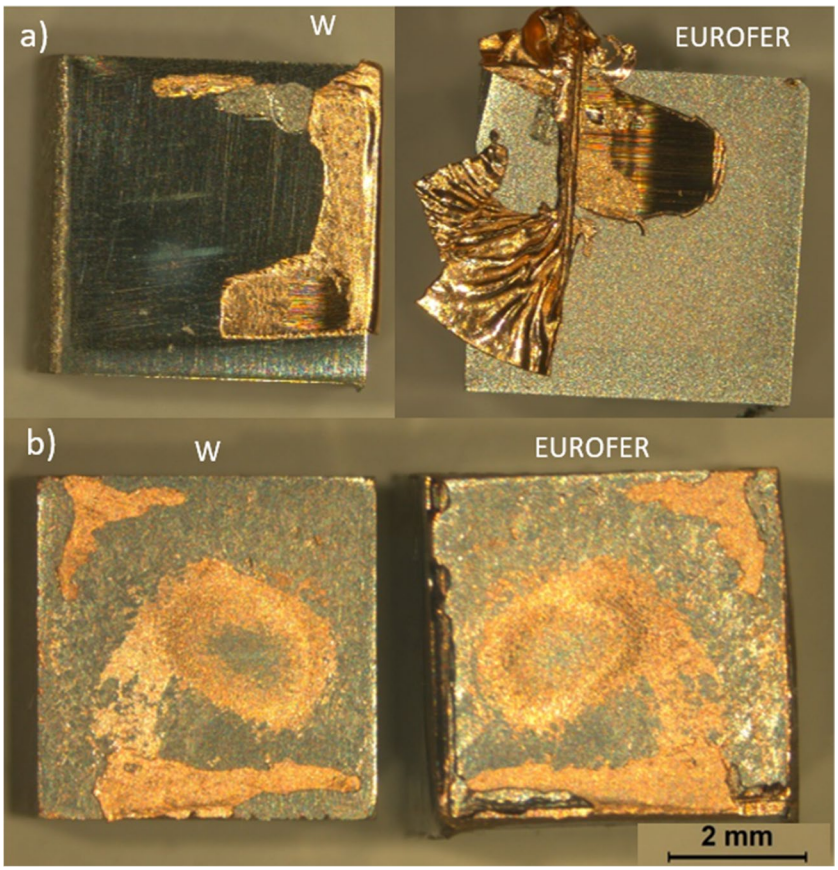

Fig. 14 Fracture surface of brazing sample of **a** 1110 °C-1 min and **b** 1110 °C-3 min

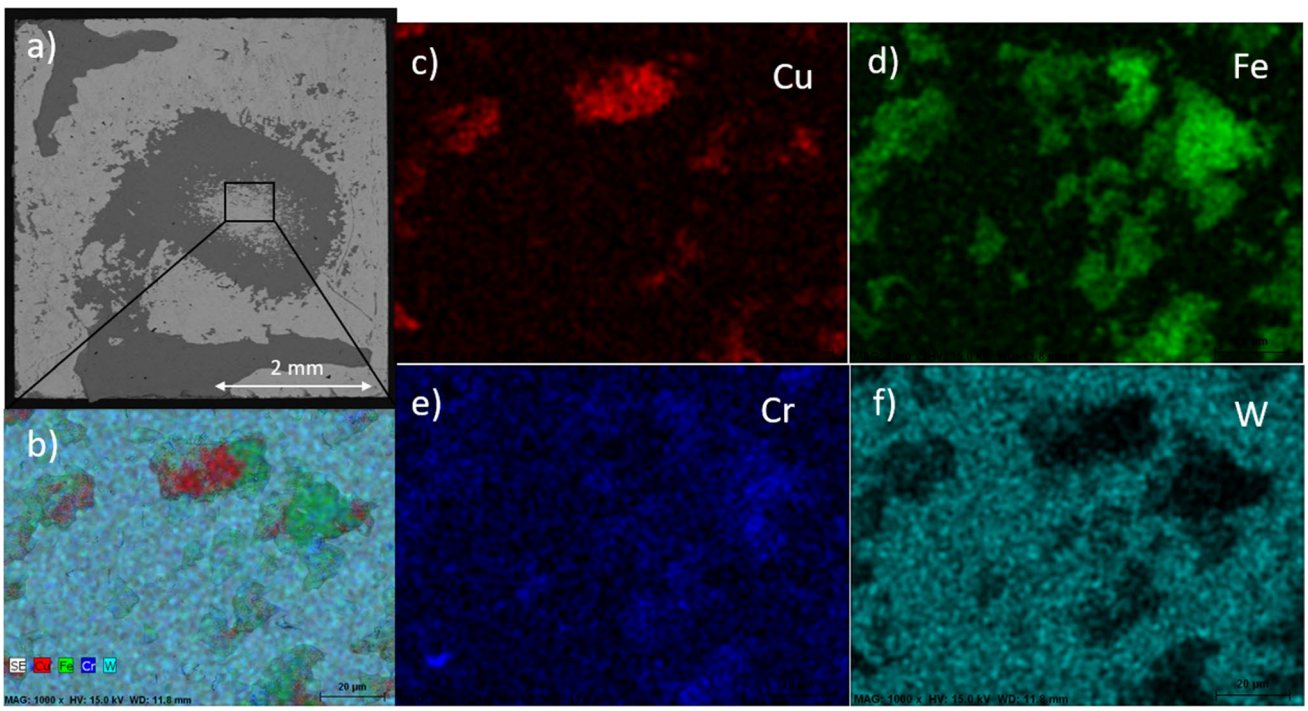

Fig. 15 Fracture surface of tungsten side of 1110 °C-3 min: **a** general view, **b** EDX analysis of a detail of the tungsten zone, and **c**–f elemental distribution map of Cu, Fe, Cr, and W, respectively

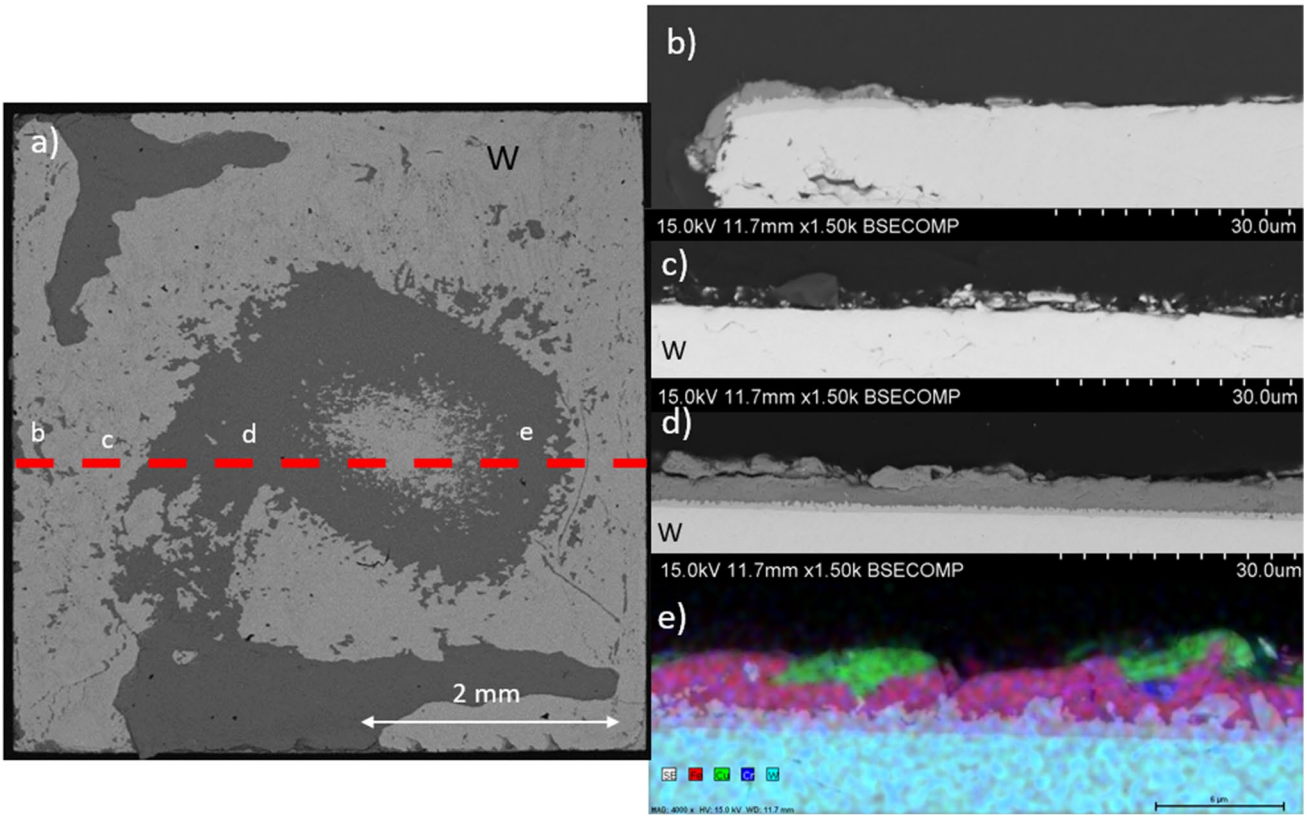

Fig. 16 **A** Fracture surfaces of samples of 1110 °C-3 min. Cross section images obtained by SEM of the fracture surfaces following the depicted line in **b**–**d** W base material and **e** elemental distribution map of W base material

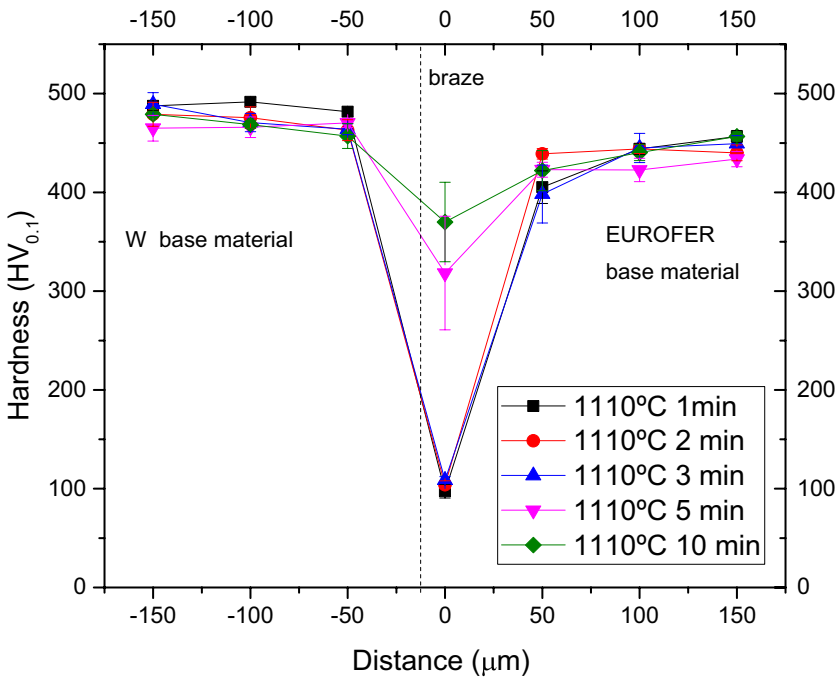

Fig. 17 Vickers microhardness profiles of W-EUROFER joints of the different conditions evaluated

show a modification in the fracture mechanism, where crack propagate through the braze and adhered copper could be observed in both fracture surfaces in Fig. 14b.

Fracture surfaces of the base materials after the shear tests were analyzed by SEM to determine the fracture mechanisms. The study of the tungsten side showed the presence of copper and some iron coming from the EUROFER, in addition to the tungsten from the base material, which indicated that crack probably has propagated following different paths during the fracture (Fig. 15a and b). The adhered EUROFER has been detached during the fracture, indicating the high adhesion properties achieved by joining those material using these conditions.

In order to study the fracture and crack propagation mechanism, cross section of W side marked with a red dash line in Fig. 16a were metallography prepared. This cross section observation allows us to study the propagation paths of the crack during the fracture. The analysis from one side to the other of the sample indicated that, at the edges of the samples, crack propagates following the interface formed by the tungsten-diffusion layer interface. Then, when the crack reaches the inner dark ring at the backscattering image, the crack propagation shifted to the interface formed by the steel band with the copper band as EDX elemental mapping distribution shown in Fig. 16e. Finally, crack propagation shifted back to the tungsten-diffusion layer until reaches the other edge.

3.3.2 Microhardness test

The microhardness profile of the brazed joints shown in Fig. 17 allows evaluating possible microstructural or mechanical changes in the base materials of the joint after the brazing process compared to the as received properties.

With respect to W, the hardness is not affected by the brazing process and it keeps close to 450 HV, which correspond to the hardness of rolled polycrystalline tungsten [29].

Concerning EUROFER, hardness values approaching 440 HV were consistently observed under various conditions, signifying a substantial hardening effect from the initial 220 HV in its as-received state [25]. These elevated hardness levels arise from alterations in the microstructure induced during thermal processes, particularly the austenitization of the steel above 890 °C, followed by rapid cooling to room temperature at rates of 5 °C/min. The employed cooling rate is high enough to transform austenite into martensite. To restore the original hardness characteristic of the as-received state, a tempering treatment at 760 °C for 90 min is indispensable. This treatment serves the dual purpose of alleviating residual stresses and converting martensite into tempered martensite, ultimately leading to the formation of the ferritic-martensitic microstructure characteristic of EUROFER [25].

Finally, differences in the hardness value in the braze area was observed. This phenomenon is directly associated with the thickness of the copper band, which decreased as the brazing time increased, reaching a point where it is not formed, and only dispersed copper zones are surrounded by EUROFER and the Fe-rich band. As a result, the hardness increases.

4 Conclusions

The wetting behavior and microstructural evolution of Cu on EUROFER and tungsten base materials were analyzed to identify optimal brazing conditions for wetting and desired microstructure. The critical microstructural changes at brazing temperature necessitate a thorough understanding of formation and evolution mechanisms due to their significant impact on mechanical properties.

Wettability studies revealed copper drops forming at 1105 °C, exhibiting superior spreading on EUROFER compared to tungsten. Enhanced copper wetting on EUROFER is linked to an active wetting behavior, involving interactions between copper and iron at the joint interface. In contrast, the Cu-W system behaves as an inert interface with no observed diffusion or interfacial reactions. Results indicate contact angles of 10° and 70° for Cu-EUROFER and Cu-W, respectively, upon reaching equilibrium.

The analysis of brazeability revealed that achieving highly continuous metallic interfaces is only feasible at 1110 °C. Significant microstructural variations were noted within the temperature range of 1 to 10 min. In the initial moments, copper incorporation into EUROFER grain boundaries and iron dilution into the braze material occurred. Moreover, an increase in iron concentration in copper led to heterogeneous precipitation in contact with tungsten, forming a continuous layer when dwell times exceeded 5 min. The W-braze interface is further characterized by the formation of a diffusion layer with W-Fe–Cr composition.

Optimal shear strength results were obtained at 1110 °C for 3 min. These brazing parameters facilitated sufficient interfacial interaction, enhancing adhesion properties and controlling the growth of the diffusion layer and the Fe-rich phase. Additionally, the copper braze maintained a continuous layer, serving as a stress-relieving phase during operation.

The brazing process did not thermally affect the W base material, whereas EUROFER underwent a hardening process associated with the formation of untempering martensite. However, this hardening effect can be restored through the application of a tempering treatment.

Author contribution I. Izaguirre: methodology, validation, formal analysis, investigation, data curation, writing—original draft, visualization. J. de Prado: methodology, validation, formal analysis, investigation, data curation, writing—original draft, visualization. M. Sánchez: conceptualization, formal analysis, investigation, resources, writing—review and editing, visualization, supervision, project administration, funding acquisition. A. Ureña: conceptualization, formal analysis, investigation, resources, writing—review and editing, visualization, supervision, project administration, funding acquisition.

Funding Open Access funding provided thanks to the CRUE-CSIC agreement with Springer Nature. This work has been carried out within the framework of the EUROfusion Consortium, funded by the European Union via the Euratom Research and Training Programme (Grant Agreement No 101052200 — EUROfusion). Views and opinions expressed are however those of the author(s) only and do not necessarily reflect those of the European Union or the European Commission. Neither the European Union nor the European Commission can be held responsible for them.

Declarations

Competing interests The authors declare the following financial interests/personal relationships which may be considered as potential competing interests: Ignacio Izaguirre reports financial support was provided by Rey Juan Carlos University.

References

1. Zhang X, Fu W, Lei Z, Wu S, Liang J, Li B (2023) Microstructure evolution of the W-C hard coatings using directed energy deposition on tungsten alloy surface. Surf Coat Technol 470(April):29827. https://doi.org/10.1016/j.surfcoat.2023.129827
2. Richardson M et al (2021) Technology readiness assessment of materials for DEMO in-vessel applications. J Nucl Mater 550:152906. https://doi.org/10.1016/j.jnucmat.2021.152906
3. Li Y, Chen C, Yi R, Ouyang Y (2020) Review: special brazing and soldering. J Manuf Process 60(October):608–635. https://doi.org/10.1016/j.jmapro.2020.10.049
4. Bachurina D et al (2021) Joining tungsten with steel for DEMO: simultaneous brazing by Cu-Ti amorphous foils and heat treatment. Fusion Eng Des 162(July 2020):112099. https://doi.org/10.1016/j.fusengdes.2020.112099
5. Mir FA, Khan NZ, Siddiquee AN, Parvez S (2022) Friction based solid state welding – a review. Mater Today Proc 62:55–62, 2022. https://doi.org/10.1016/j.matpr.2022.01.457
6. Kaptay G (2008) A unified model for the cohesive enthalpy, critical temperature, surface tension and volume thermal expansion coefficient of liquid metals of bcc, fcc and hcp crystals. Mater Sci Eng A 495(1–2):19–26. https://doi.org/10.1016/j.msea.2007.10.112
7. Kaptay G (2020) A coherent set of model equations for various surface and interface energies in systems with liquid and solid metals and alloys. Adv Colloid Interface Sci 283:102212. https://doi.org/10.1016/j.cis.2020.102212
8. Liu P, Qian X, Mao X, Song W, Peng X (2020) Study on creep-fatigue of heat sink in W/CuCrZr divertor target based on a new approach to creep life. Nucl Mater Energy 25:100846. https://doi.org/10.1016/j.nme.2020.100846
9. Chen Y et al (2021) High-strength diffusion bonding of oxide-dispersion-strengthened tungsten and CuCrZr alloy through surface nano-activation and Cu plating. J Mater Sci Technol 92:186–194. https://doi.org/10.1016/j.jmst.2021.03.040
10. Li K, Shan J, Wang C, Tian Z (2017) The role of copper in microstructures and mechanical properties of laser-welded Fe-19Ni-3Mo-1.5Ti maraging steel joint. Mater Sci Eng A 681(October 2016):41–49. https://doi.org/10.1016/j.msea.2016.10.039
11. Zhang Y, Galloway A, Wood J, Robbie MBO, Easton D, Zhu W (2014) Interfacial metallurgy study of brazed joints between tungsten and fusion related materials for divertor design. J Nucl Mater 454(1–3):207–216. https://doi.org/10.1016/j.jnucmat.2014.07.058
12. Bachurina D et al (2019) High-temperature brazing of tungsten with steel by Cu-based ribbon brazing alloys for DEMO. Fusion Eng Des 146(February):1343–1346. https://doi.org/10.1016/j.fusengdes.2019.02.072
13. de Prado J, Sánchez M, Ruiz A, Ureña A (2020) Effect of brazing temperature, filler thickness and post brazing heat treatment on the microstructure and mechanical properties of W-Eurofer joints brazed with Cu interlayers. J Nucl Mater 533:152117. https://doi.org/10.1016/j.jnucmat.2020.152117
14. Seltzman AH, Wukitch SJ (2022) Brazing characteristics, microstructure, and wettability of laser powder bed fusion additive manufactured GRCop-84 compared to CuCrZr and OFC, and brazing to titanium-zirconium-molybdenum alloy limiters. Fusion Eng Des 180(February):113185. https://doi.org/10.1016/j.fusengdes.2022.113185
15. Li Y, Wang C, Li X, Zhang L, Pan P, Lei M (2023) Brazing YAG ceramic to Kovar alloy with Ag–Cu–Ti filler alloy: wettability, microstructure and mechanical properties. Vacuum 213(April):112093. https://doi.org/10.1016/j.vacuum.2023.112093
16. Binesh B (2020) Diffusion brazing of IN718/AISI 316L dissimilar joint: Microstructure evolution and mechanical properties. J Manuf Process 57(April):196–208. https://doi.org/10.1016/j.jmapro.2020.06.025
17. Jiang CY, Li XQ, Wan B, Zhu DZ, Qu SG, Yang C (2022) Microstructure evolution and mechanical properties of TiAl/GH536 joints vacuum brazed with Ti–Zr–Cu–Ni filler metal. Intermetallics 142(December 2021):107468. https://doi.org/10.1016/j.intermet.2022.107468
18. Paidar M, Ashraff Ali KS, Ojo OO, Mohanavel V, Vairamuthu J, Ravichandran M (2021) Diffusion brazing of Inconel 617 and 321 stainless steel by using AMS 4772 Ag interlayer. J Manuf Process 61(October 2020):383–395. https://doi.org/10.1016/j.jmapro.2020.11.013
19. Mergia K, Boukos N (2008) Structural, thermal, electrical and magnetic properties of Eurofer 97 steel. J Nucl Mater 373(1–3):1–8. https://doi.org/10.1016/j.jnucmat.2007.03.267
20. de Prado J, Sánchez M, Utrilla MV, López MD, Ureña A (2016) Study of a novel brazing process for W-W joints in fusion applications. Mater Des 112:117–123. https://doi.org/10.1016/j.matdes.2016.09.067
21. Varanasi D, Szabo JT, Baumli P (2019) Investigation of the copper penetration and joint microstructure observed in low alloyed

steels. NanoWorld J 5(3):36–40. https://doi.org/10.17756/nwj.2019-070
22. Daehn KE, Serrenho AC, Allwood J (2019) Preventing wetting between liquid copper and solid steel: a simple extraction technique. Metall Mater Trans B Process Metall Mater Process Sci 50(4):1637–1651. https://doi.org/10.1007/s11663-019-01578-0
23. Somlyai-Sipos L, Baumli P (2022) Wettability of metals by water. Metals (Basel) 12(8). https://doi.org/10.3390/met12081274
24. Kaptay G (2016) Modelling equilibrium grain boundary segregation, grain boundary energy and grain boundary segregation transition by the extended Butler equation. J Mater Sci 51(4):1738–1755. https://doi.org/10.1007/s10853-015-9533-8
25. Cui S, Jung IH (2017) Thermodynamic modeling of the Cu-Fe-Cr and Cu-Fe-Mn systems. Calphad Comput Coupling Phase Diagrams Thermochem 56(November 2016):241–259. https://doi.org/10.1016/j.calphad.2017.01.004
26. A. S. M. International (1989) Alloy Phase Diagram 10(2)
27. Rieth M et al (2003) EUROFER 97 tensile, charpy, creep and structural tests. Meas J Int Meas Confed 140:142–150
28. Li H, Ma T, He Y, Li Y (2022) Research on the diffusion behavior of Cu in low-carbon steel under high temperatures. Crystals 12(2). https://doi.org/10.3390/cryst12020207
29. Kim HC et al (2021) Analysis of hardness and microstructural changes in tungsten mono-blocks exposed to high heat flux at 10 MW/m2. Fusion Eng Des 170(April):112530. https://doi.org/10.1016/j.fusengdes.2021.112530